Electronic Supplementary Material (ESI) for Lab on a Chip.

Tough, Permeable and Biocompatible Microfluidic Devices Formed through the Buckling Delamination of Soft Hydrogel Films

Riku Takahashi[a, *], Hiroki Miyazako[a, †], Aya Tanaka[a], Yuko Ueno[a, ‡] & Masumi Yamaguchi[a]

[a.] *NTT Basic Research Laboratories, Bio-Medical Informatics Research Center, NTT Corporation, 3-1 Morinosato -Wakamiya, Atsugi, Kanagawa, 243-0198, Japan.*

[*.] *Corresponding author: riku.takahashi.fv@hco.ntt.co.jp*

[†.] *Current address: Department of Information Physics and Computing, Graduate School of Information Science and Technology, The University of Tokyo, Tokyo, Japan.*

[‡.] *Current address: Department of Applied Chemistry, Faculty of Science and Engineering, Chuo University, Tokyo, Japan.*

Supplementary Information

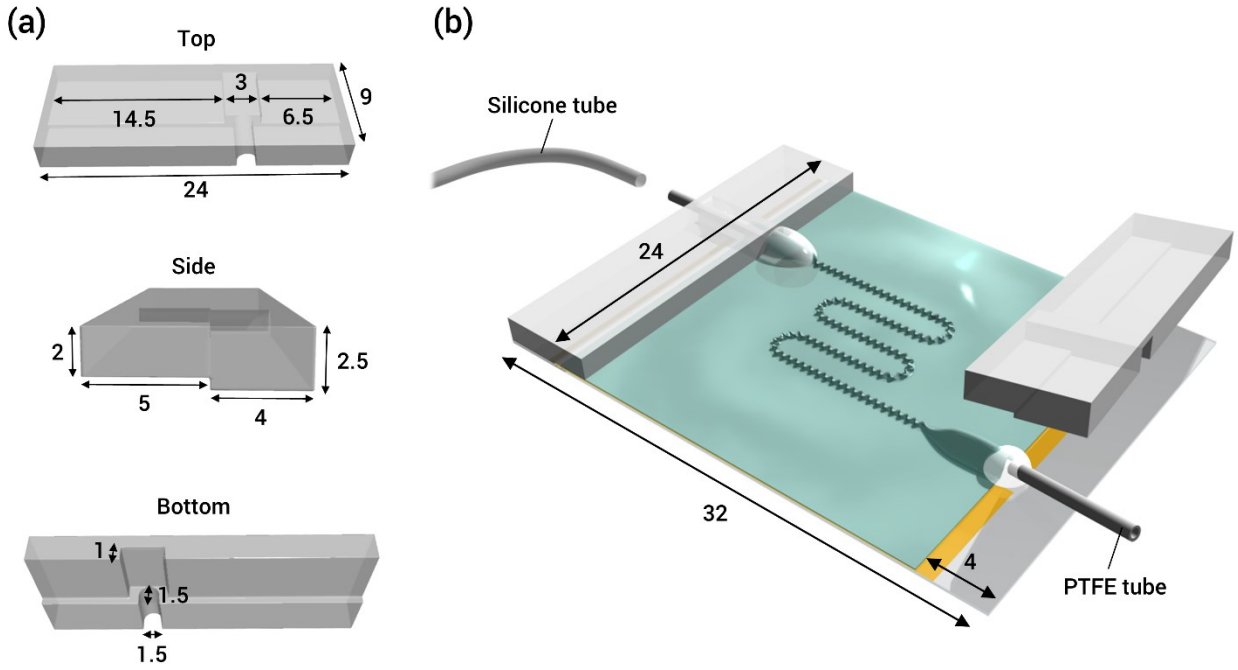

Supplementary Figure S1

Fig. S1. Geometries of the 3D printed connecter and microfluidic device. a) Schematic illustration of the 3D printed connecter viewed from top, side, and bottom. b) Schematic illustration of the microfluidic device. The connecters were secured at a predetermined place with adhesive glue. Outer and inner diameters of the PTFE tubes are 1.5 and 0.5 mm, respectively. Outer and inner diameters of the silicone tubes are 1.5 and 1.0 mm, respectively. Values in (a) and (b) are dimensions of the connecter and device (unit: mm).

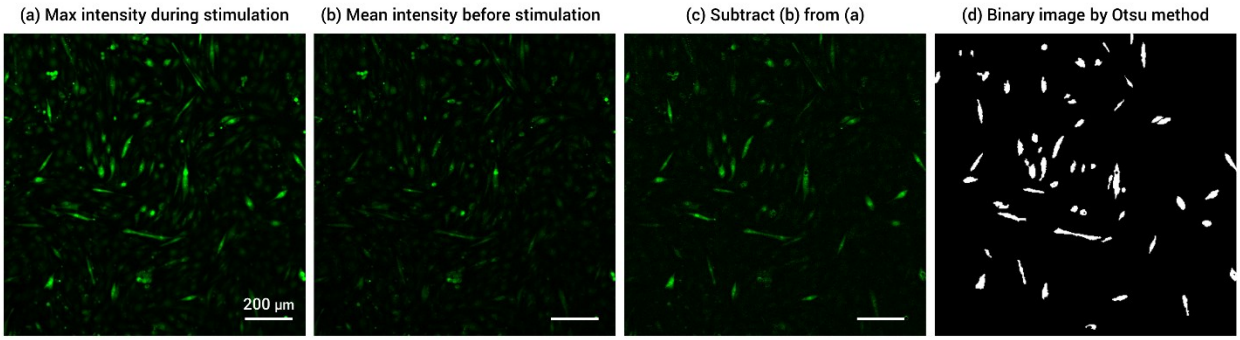

Supplementary Figure S2

Fig. S2. Method for defining region of interest (ROI) to quantify fluorescence intensity change of ACh-active myotubes. (a) Maximum fluorescence intensity during chemical stimulation was abstracted from series of images by ImageJ. (Image → Stacks → Z Projection → Max Intensity). (b) Mean intensity before chemical stimulation was obtained as background by ImageJ (Image → Stacks → Z Projection → Average Intensity). (c) To characterize the ACh-active myotubes, the subtracted image was obtained by processing (a) and (b) via ImageJ (Process → Image Calculator → Operation → Subtract). High-intensity region in this image represents "stimulated cells". (d) To make ROIs, the intensity color image (c) was converted to a binary image (d) with a threshold determined by the Otsu method. After that, outlines of cells were captured by a wand tool as the ROIs.

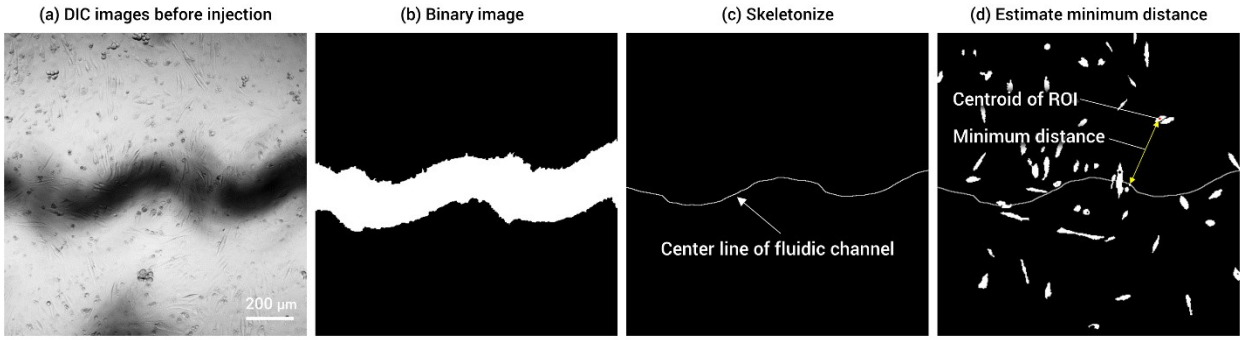

Supplementary Figure S3

Fig. S3. Method for determining distance between cells (ROIs) and the microchannel. a) DIC image before chemical injection clearly shows the position of the microchannel as a black shadow. (b) To define the channel outline, the DIC image (a) was converted to a binary image (b) with a threshold determined by the Otsu method. (c) To show the center line of the microchannel, the binary image (b) was skeletonized by ImageJ (Process → Binary → Skeletonize). (d) From the centerline of the microchannel in image (c) and the binary image of ACh-activated myotubes [Fig. S2(d)], minimum distances between the centroid of each ROI and the centerline were obtained.

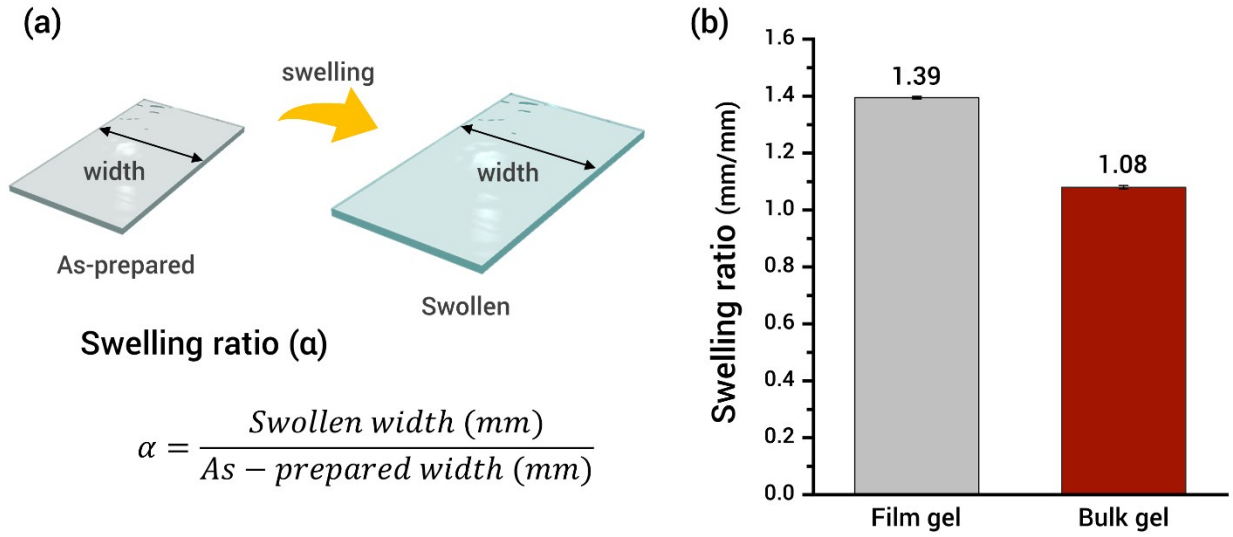

Supplementary Figure S4

Fig. S4. (a) Swelling ratios of film PAAm gel (4M monomer, 0.012M cross-linker, and 0.004M initiator) and the bulk PAAm gel (1.5M monomer, 0.03M cross-linker, and 0.0015M initiator) were estimated from the swollen width divided by the as-prepared width. For this experiment, the as-prepared size of the gel was fixed as 20-mm length, 10-mm width, and 0.5-mm-thickness. (b) Calculated swelling ratios. The gray and red bars represent the film gel and bulk gel, respectively. Inset values suggest the size change ratios, which are ~39% and ~8% for the film gel and bulk gel, respectively. The error bars are standard deviations obtained from results for three samples.

Supplementary Figure S5

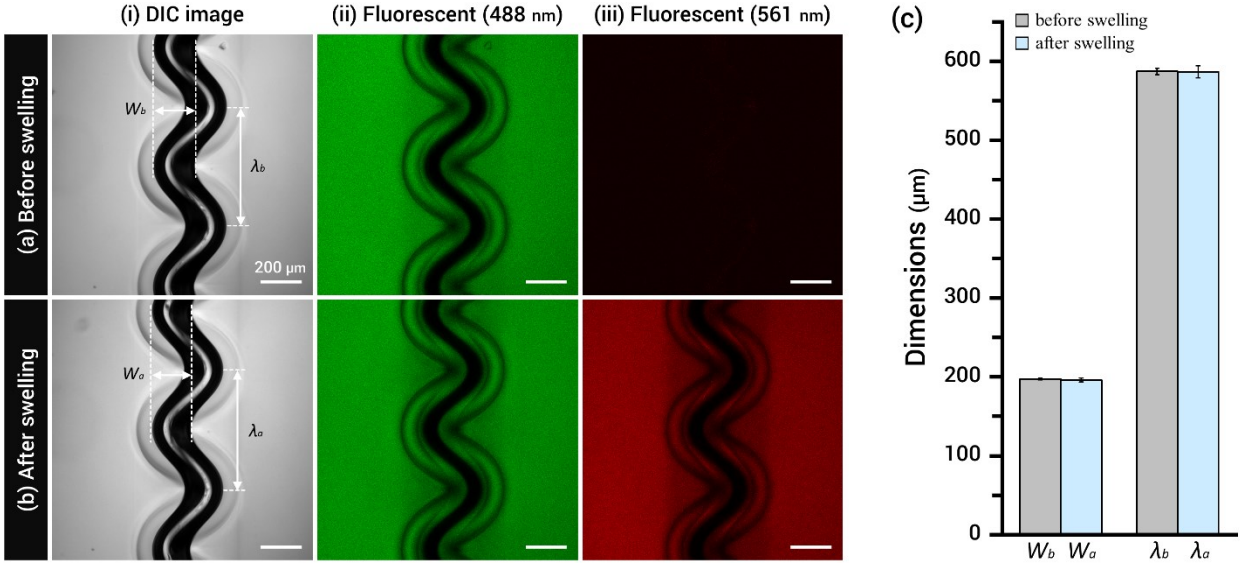

Fig. S5. Size changes in single-film devices during swelling in the bulk gel solution. (a,b) DIC and fluorescent images of (a) before and (b) after swelling. The single-film devices were labeled by 0.05wt% FL and the bulk gel solution contained 0.05% RB. Swelling time was the same as in the method for stacking bulk gels (3 min). (c) From the images in (a) and (b), width ($W_{b,a}$), and period ($\lambda_{b,a}$) of microchannels were measured. Subscripts *b* and *a* represent the before and after swelling, respectively. The data are presented in (c) as mean ± S. D. (n=3).

Supplementary Figure S6

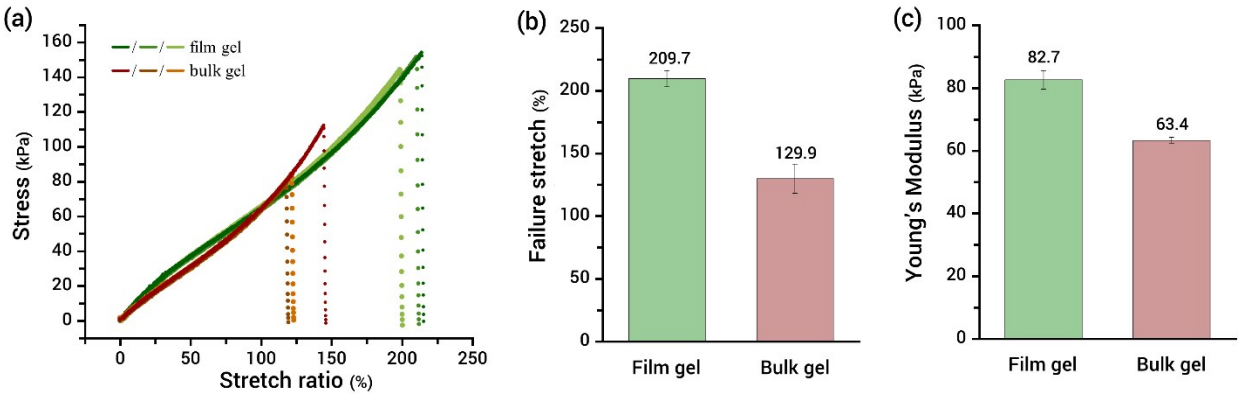

Fig. S6. Mechanical properties of film and bulk PAAm gels. (a) Tensile stress-strain curves of film (green) and bulk (red) PAAm gels. Both samples were prepared with the dimensions 12×2×0.75 mm; 12 mm was the gauge length. All the samples were stretched along their length direction at an extension rate of 100 mm/min using a tensile-compressive tester (STB-1225S, A&D Co. Ltd.). The tensile stretch ratio, λ, is defined as $l/l_0 \times 100$, where l_0 and l are the lengths of the gel before and during elongation, respectively. Three representative data sets are presented for both gels. (b) Failure stretch ratios of film (green) and bulk (red) PAAm gels. (c) Young's modulus of film (green) and bulk (red) PAAm gels, estimated from initial slope of stress-strain curves. The error bars in (b) and (c) are standard deviations obtained from results for three samples.

Supplementary Figure S7

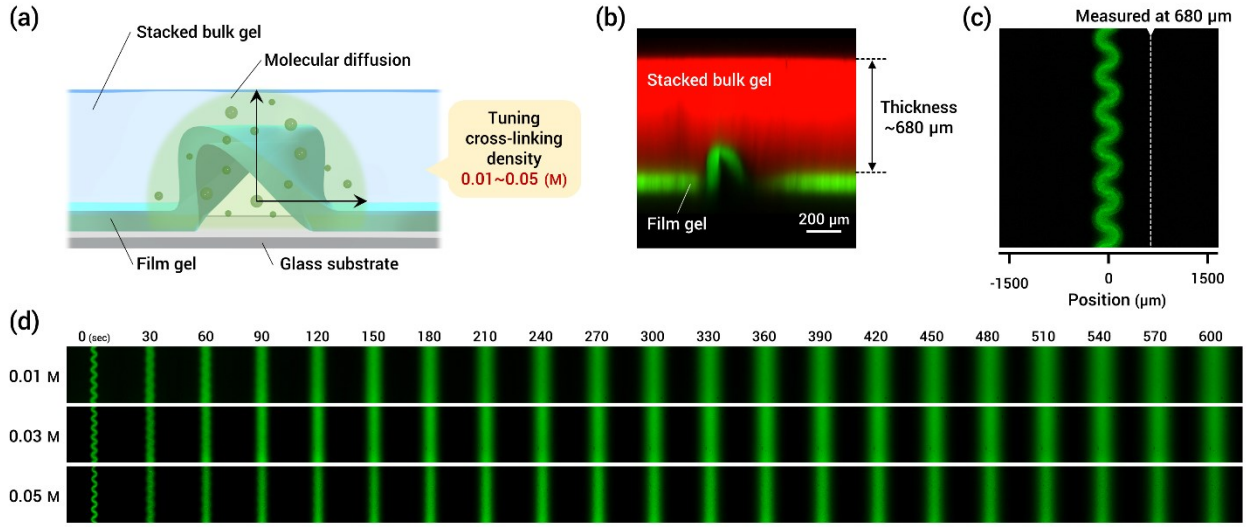

Fig. S7. How the fluorescence intensity is quantified to estimate the penetration time for chemicals from microchannels to the surface of the stacked bulk gels. (a) Schematic illustration of diffusion of chemicals from microchannels, assuming that lateral diffusion behavior is the same in the thickness direction. (b) Thickness of the stacked bulk gel obtained from 3D architecture characterization in Fig. 2(d). (c) Position of analyzed line for quantifying the fluorescence intensity. (d) Time-lapse fluorescence images of uranine (10 mM) diffusion from microchannel (injection volume: 20 μL). To characterize the diffusivity over the composition of bulk PAAm gels, cross-linker concentration was varied from 0.01M to 0.05M.

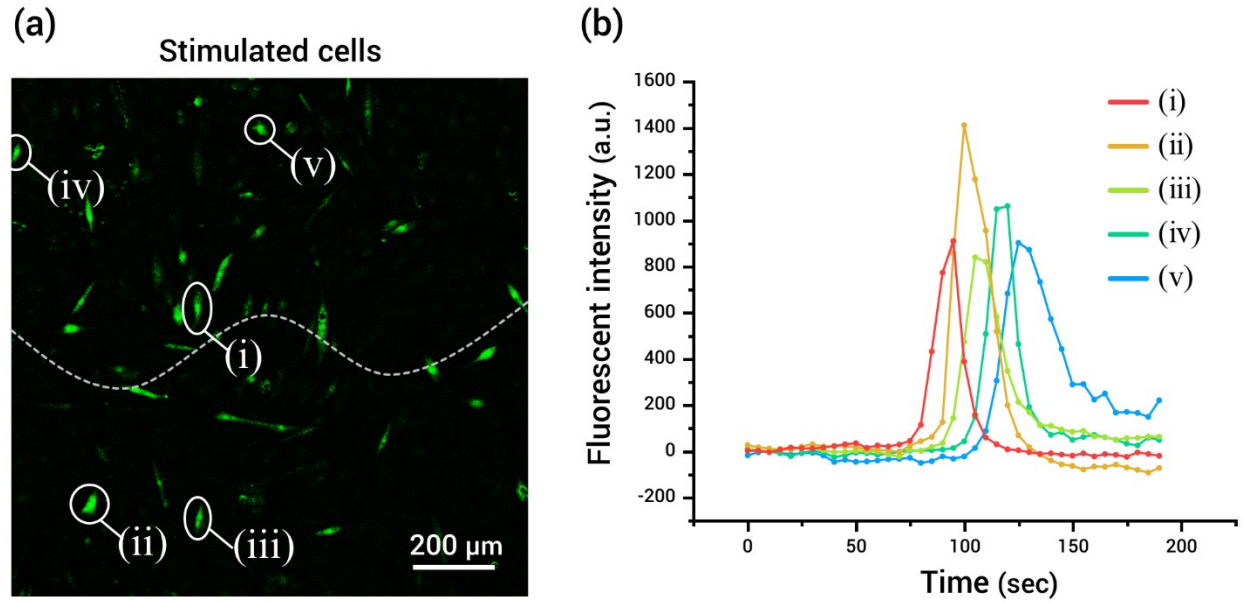

Supplementary Figure S8

Fig. S8. Fluorescence intensity plots during chemical stimulation. (a) Stimulated cells image obtained as shown Fig. S2(c). White circles and white dashed line represent quantified cells and the centerline of the microchannel, respectively. b) Representative plots of fluorescence intensity during chemical stimulation.

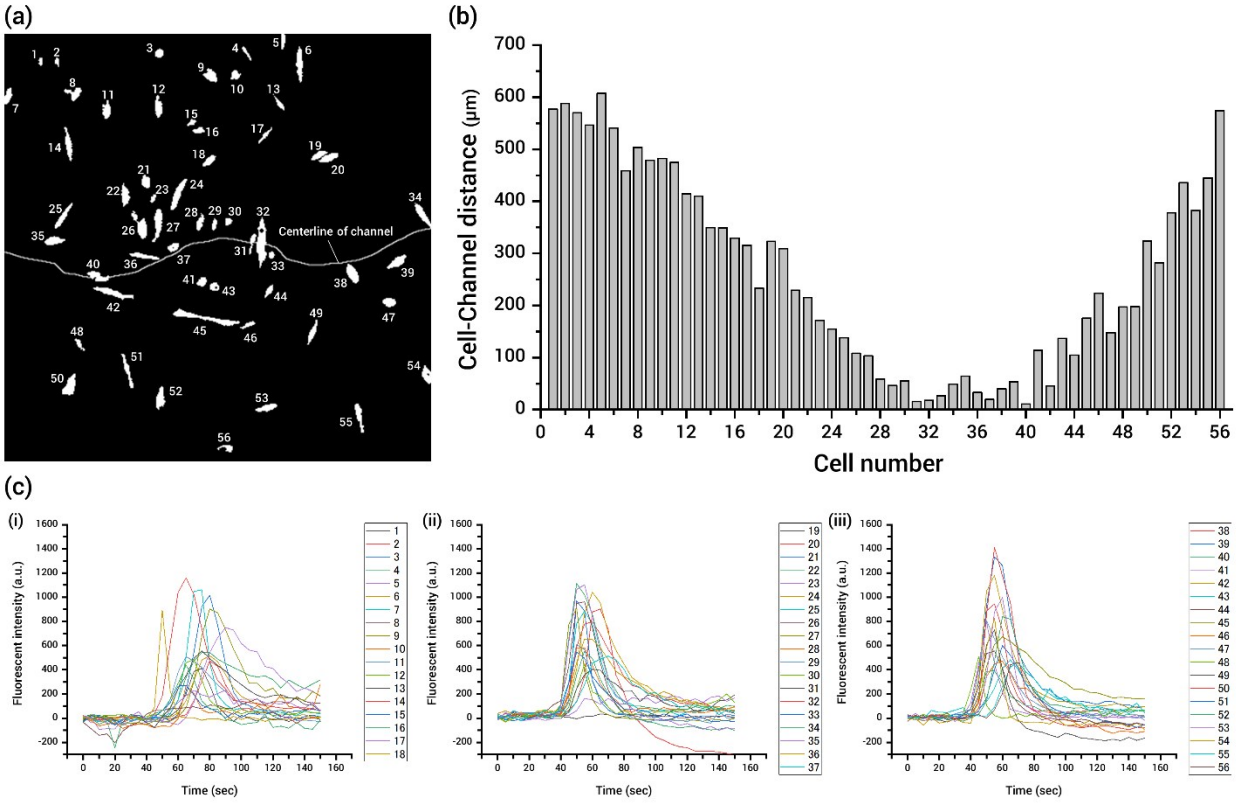

Supplementary Figure S9

Fig. S9. Quantification of cell-channel distance and fluorescence intensity plot for all stimulated cells. (a) ROIs (stimulated cells) are assigned numbers (1-56) to identify each cell. (b) Minimum distances between centroid of each ROI and centerline of the microchannel. (c) Fluorescence intensity plots of all ROIs during chemical stimulation. To visualize all the plots, we divided them into three parts: (i) 1-18, (ii) 19-37, and (iii) 38-56. Each time peak in intensity is defined as the time showing the highest intensity in the individual plots.

Supplementary Figure S10

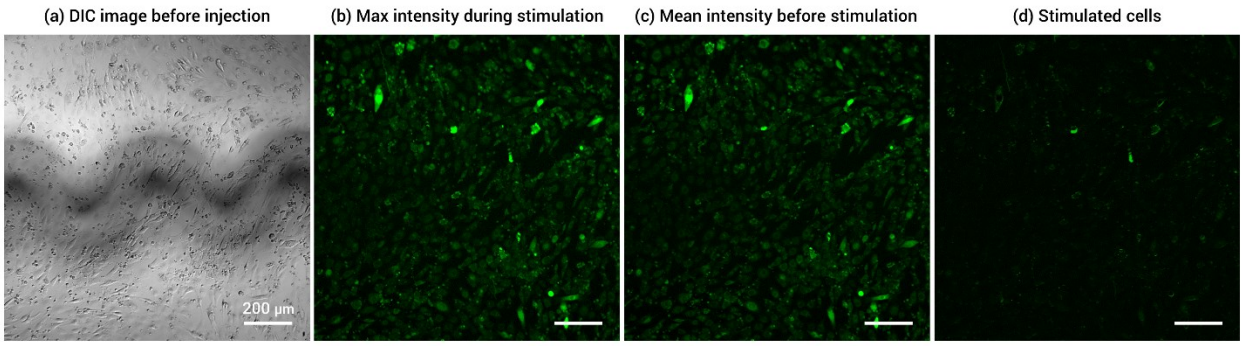

Fig. S10. Control experiment of chemical stimulation for live cells through molecular diffusion via the hydrogel matrix from the microchannel. In this experiment, 20 μL of PBS(-) solution was injected into the microchannel with a 500-μL/min flow rate. (a) DIC image before chemical injection clearly shows the position of the microchannel and live cells. (b) (c) Maximum intensity during stimulation and mean intensity before stimulation were obtained by the same procedure as described in Fig. S2. (d) Image of stimulated cells was obtained by subtracting (c) from (b). It was found that PBS(-) solution did not stimulate the live cells.

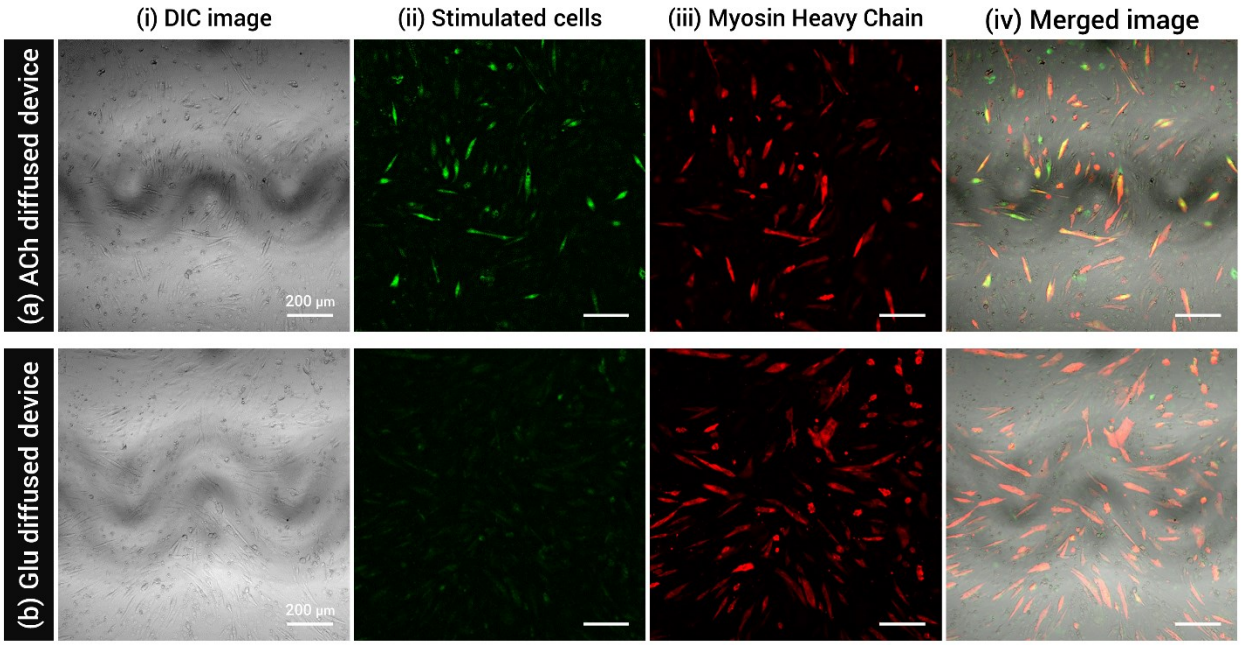

Supplementary Figure S11

Fig. S11. Immunofluoresence staining for the (a) ACh- and (b) Glu-diffused device. Experimental procedure of immunofluorescence was the same as shown in the experimental section in the main manuscript. In this experiment, Myosin 4 Monoclonal Antibody (MF20, eFluor 660) was used. From the (i) DIC images, (ii) stimulated cell image obtained from Fig. S2(c), and (iii) expression of MHC, we found that enough myotubes existed on both devices; however, stimulated cells were observed only on the ACh-diffused device. In addition, the positions of stimulated cells well agree with that of MHC expression as shown in the merged image [(a)-iv]. Therefore, we conclude that ACh molecules stimulated myotubes on the device, resulting in an increase of fluorescence intensity. On the other hand, myotubes on the device were not stimulated by Glu molecules.

Supplementary Movie 1

Real-time movie of microchannel deformation of the single-layer device. To generate air pressure, one end was sealed by adhesive glue and the other end was connected to a micropipette that can flow air manually. Here, we injected totally 200 μL of air into a 10-mm-long straight microchannel.

Supplementary Movie 2

Time-lapse observation of the fluorescence-labeled myotubes on the layer stack device during acetylcholine (ACh) solution diffusion from the microchannel. Detailed experimental conditions are described in the experimental section in the main manuscript.

Supplementary Movie 3

Time-lapse observation of the fluorescence-labeled myotubes on the layer stack device during glutamic acid (Glu) solution diffusion from the microchannel. Detailed experimental conditions are described in the experimental section in the main manuscript.